Modelling advective gas flow in compact bentonite: Lessons learnt from different numerical approaches

Mas,E.T., Harrington,J.F., Brüning,T., Shao,H., Dagher,E.E., Lee,J., Kim,K., Rutqvistm,J., Kolditz,O., Lai,S.H., Chittenden,N., Wang,Y., Damians,I.P., Olivella,S.

International Journal of Rock Mechanics and Mining Sciences **139**,104580,2021.

Advisor：Prof. Jui-Sheng Chen
Student：Yu-Sheng Lin
Date：2023/05/26

Outline

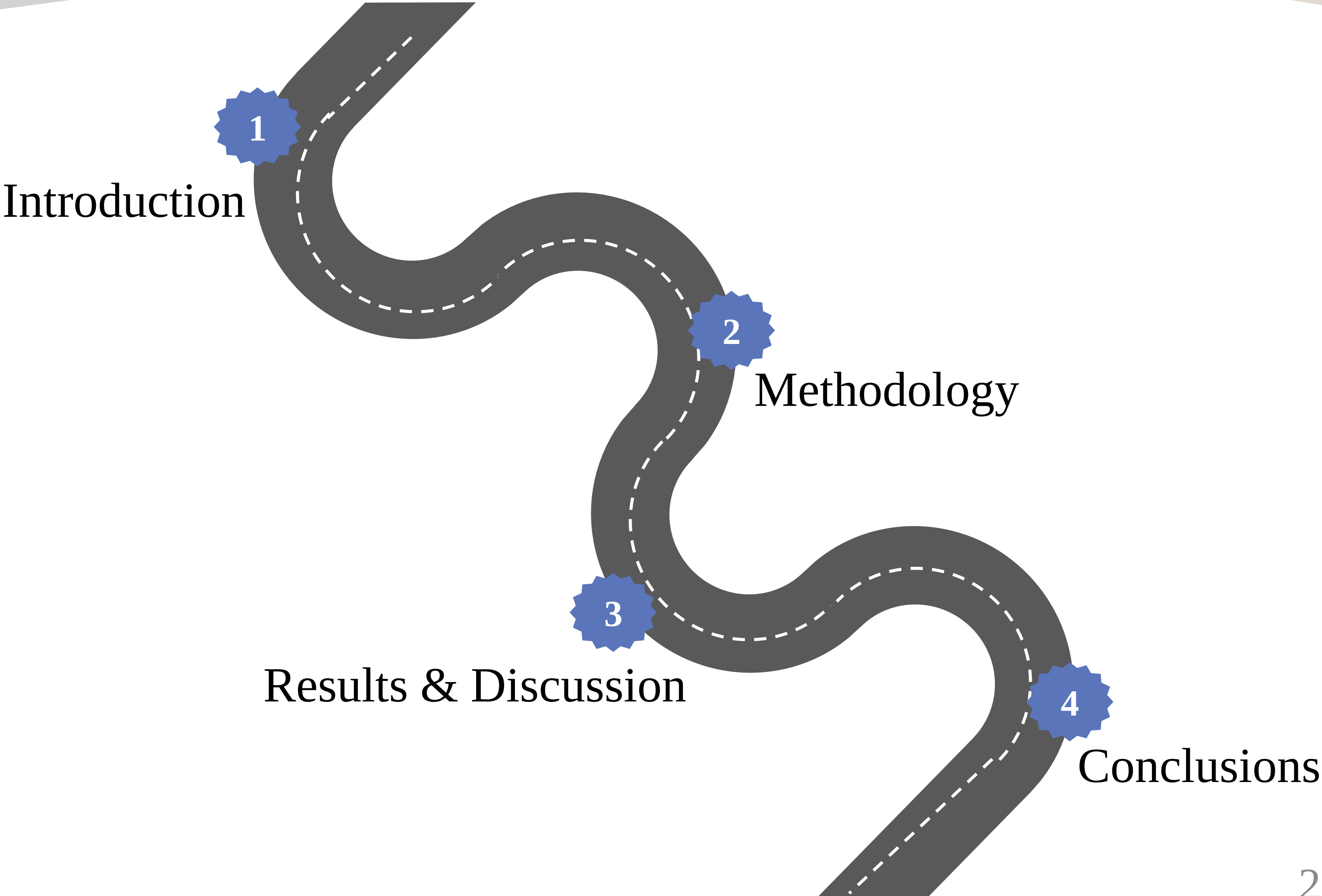
1
Introduction
2
Methodology
3
Results & Discussion
4
Conclusions

Introduction

Nuclear waste repository: Deep Geological Disposal

- Nuclear waste has high level of radioactivity and a long half-life.
- For protecting human being and ensure environmental safety. After years of international research, it is considered that "Deep Geological Disposal" is the preferred option.
- To isolate it from the biosphere, nuclear waste is buried in the geology below more than 400m, and then the canister and buffer materials are used to cover and place.

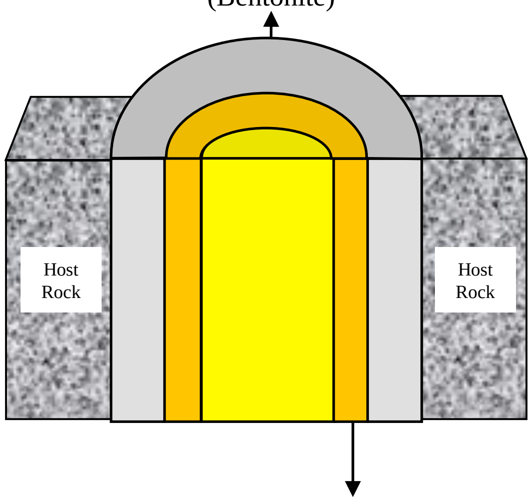

Fig.1. Schematic cross-section
(reference from Rebecca Lunn)

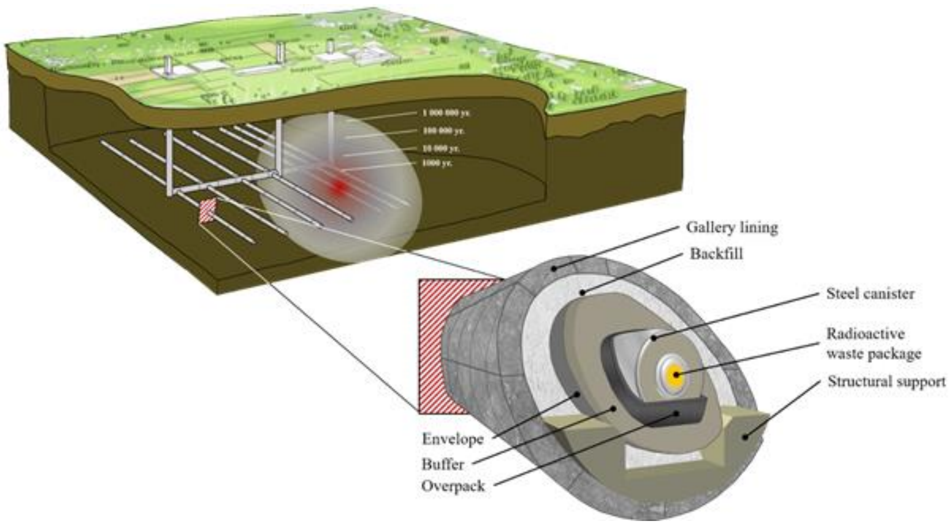

Fig.2. Design concept for the Deep Geological Disposal
(figure from Gilles Corman)

Gas migration in bentonite

- Gas may be generated due to the corrosion of metallic materials under anoxic conditions(H_2), the radioactive decay of waste(Rn) and the radiolysis of water (H_2).

When gas production rate is slow

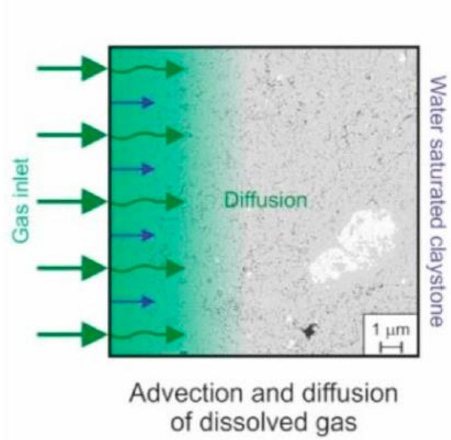

gas dissolve in porewater, and migrate by advection and diffusion

When gas production rate exceeds gas diffusion rate

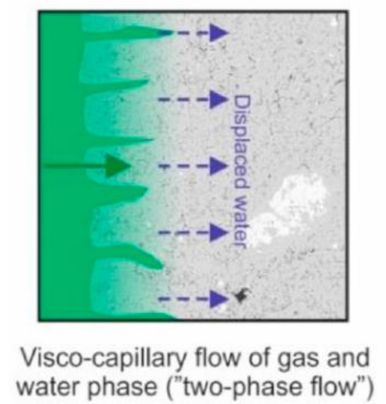

a discrete gas phase will form, parts of porewater is displaced by gas.

Gas migration in bentonite

- When gas pressure accumulates to a very high value (called gas breakthrough), gas pressure cannot withstand stress acting on the rock mass, gas might follow by pathway dilation and tensile fractures, and then escape from the bentonite.

tensile fractures

When gas pressure accumulates to a very high value

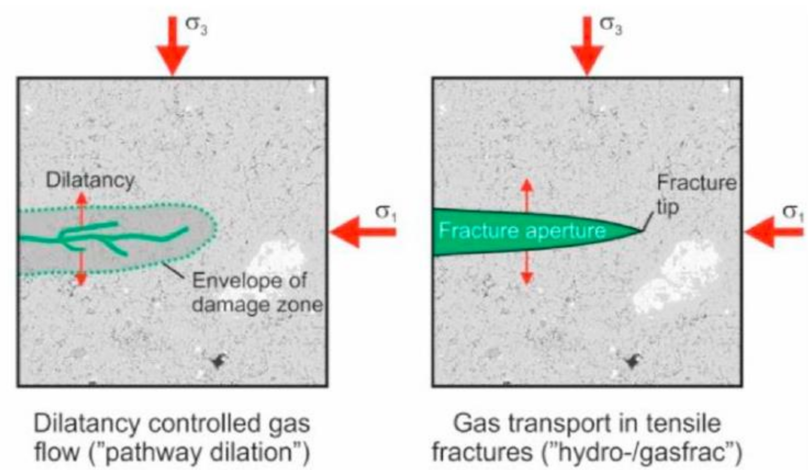

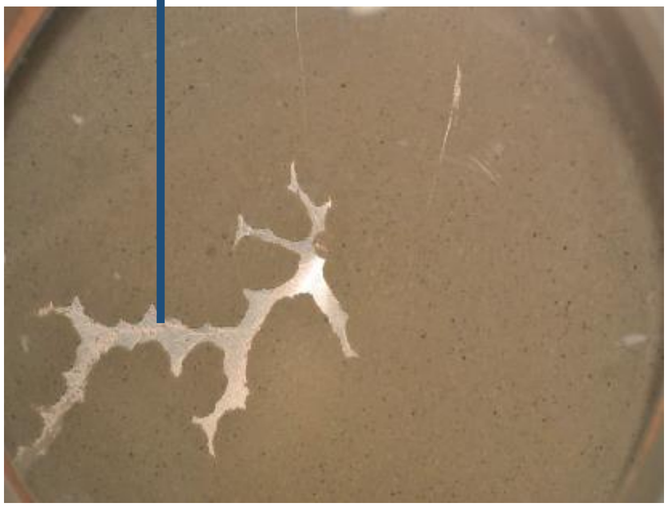

Fig.3. The mechanisms of gas migration in clays. (from Marschall et al.)

DECOVALEX-2019 project

- Therefore, gas migration in the bentonite becomes a key issue for the safety assessment of the nuclear waste disposal.
- However, the detail of the mechanisms of gas migration is unclear. Several international projects aim to understand have already been conducted.
- An international projects called DECOVALEX-2019, the Task-A is modelling gas injection experiments to develop novel numerical techniques.

Objective

To develop novel numerical techniques about gas migration. This paper summaries the outcomes of work in Task-A and a synthesis of the work of the participating modelling teams.

Experimental data

- In this task, two different gas injections experiments undertaken by the British Geological Survey (BGS) were used:
  - (a) Test-1: a 1D gas flow test
  - (b) Test-2: a 3D (spherical) gas flow test

Two different gas injections

(Test-1)

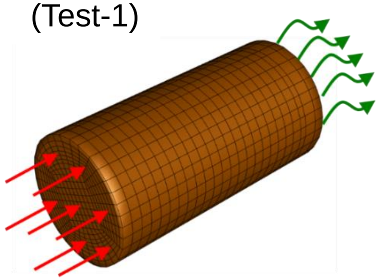

(Test-2)

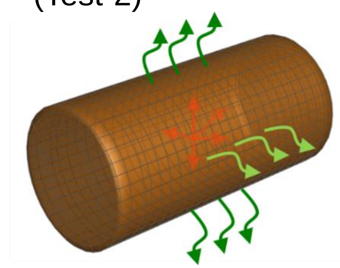

Red arrows: gas outflow emitted from the gas filters into bentonite
Green arrows: gas outflow detected by gas filters

Gas injection experiments

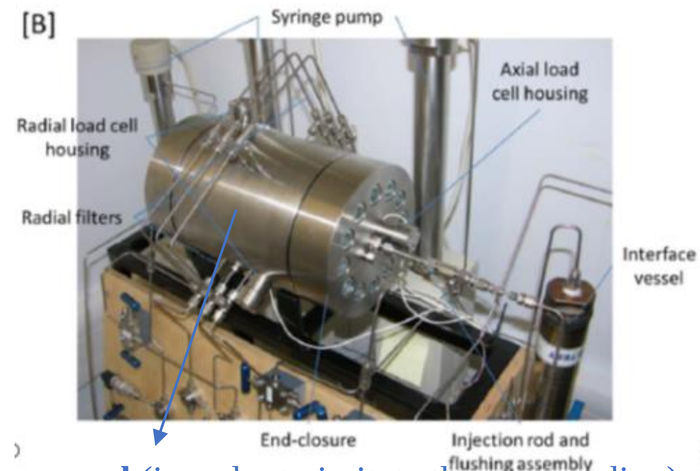

Pressure vessel (in order to imitate the surrounding) contains bentonite sample.

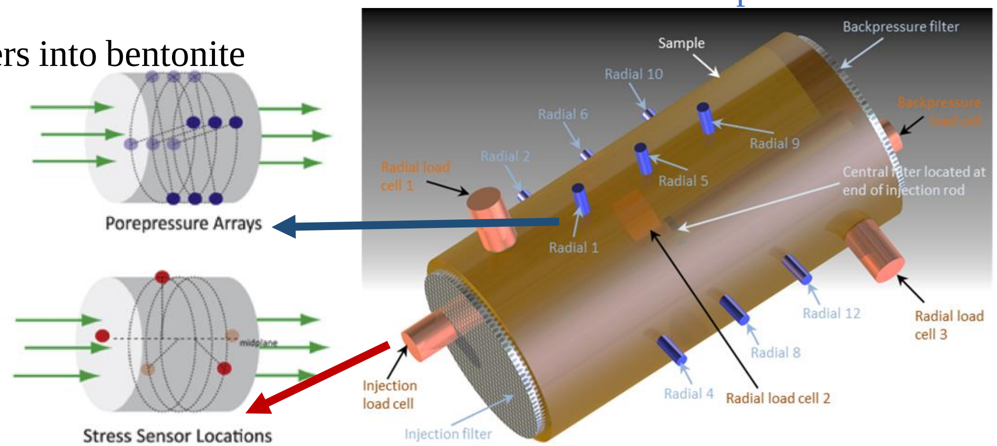

Experimental data: Test-1

Table 1
Injector schedule for the one-dimensional gas flow experiment.

Start Time (days)	Injection pump rate (μL/h)	Comments
39	0	Gas pressure: 3 MPa Initial gas volume: 235 ml
46.135	500	Start of injection pump
54.149	375	Reduce injection pump flow rate
60.959		Gas refilled (+59.95 ml, pressure maintained)
71.369	0	Injection pump stopped

Day63.8
gas breakthrough

Gas pressure decrease after breakthrough (because pathways open, then gas escape)

Day39 add additional helium and then gas pressure increase

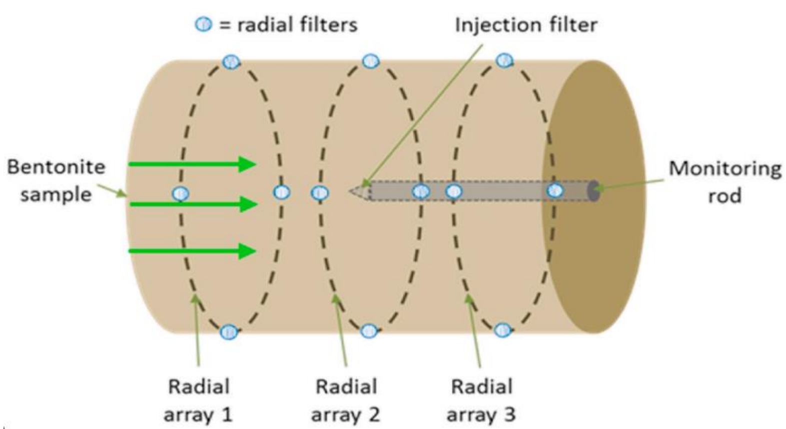

Fig.4. Schematic drawings of Test-1

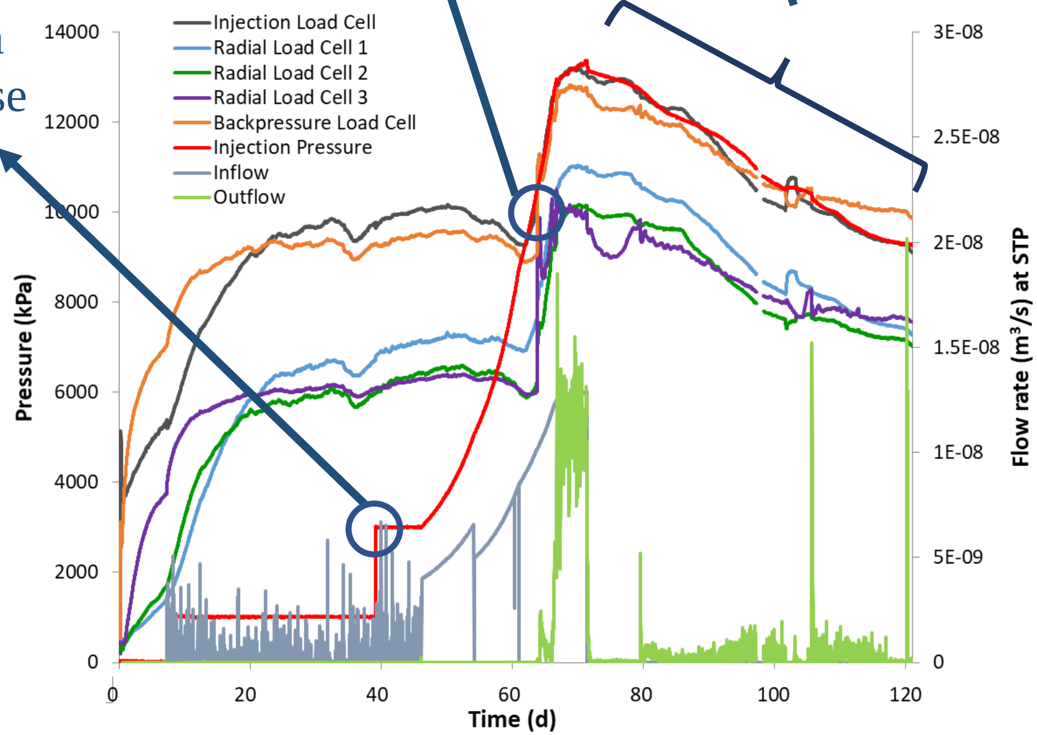

Fig.5. Experimental data from day 0 to day 120

Experimental data: Test-2

Have three times gas breakthrough events

Day757 major gas breakthrough

Start Time (days)	Injection pump rate (μL/h)	Comments
720.3	125	Gas pressure: 5 MPa Initial gas vol.: 211 ml
768.3		Gas refilled (+91.3 ml @ 9.5 MPa)
799.2		Gas refilled (+27.6 ml @ 8.7 MPa)
807.4		Gas refilled (+61.2 ml @ 8.4 MPa)
827.0		Gas refilled (+9.3 ml @ 8.3 MPa)
831.1		Gas refilled (+47.7 ml @ 8.2 MPa)

Table 2
Injector schedule for the point-injection experiment.

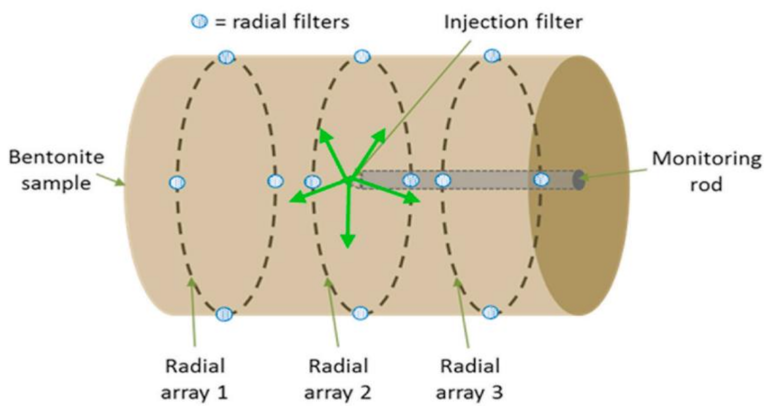

Fig.6. Schematic drawings of Test-2

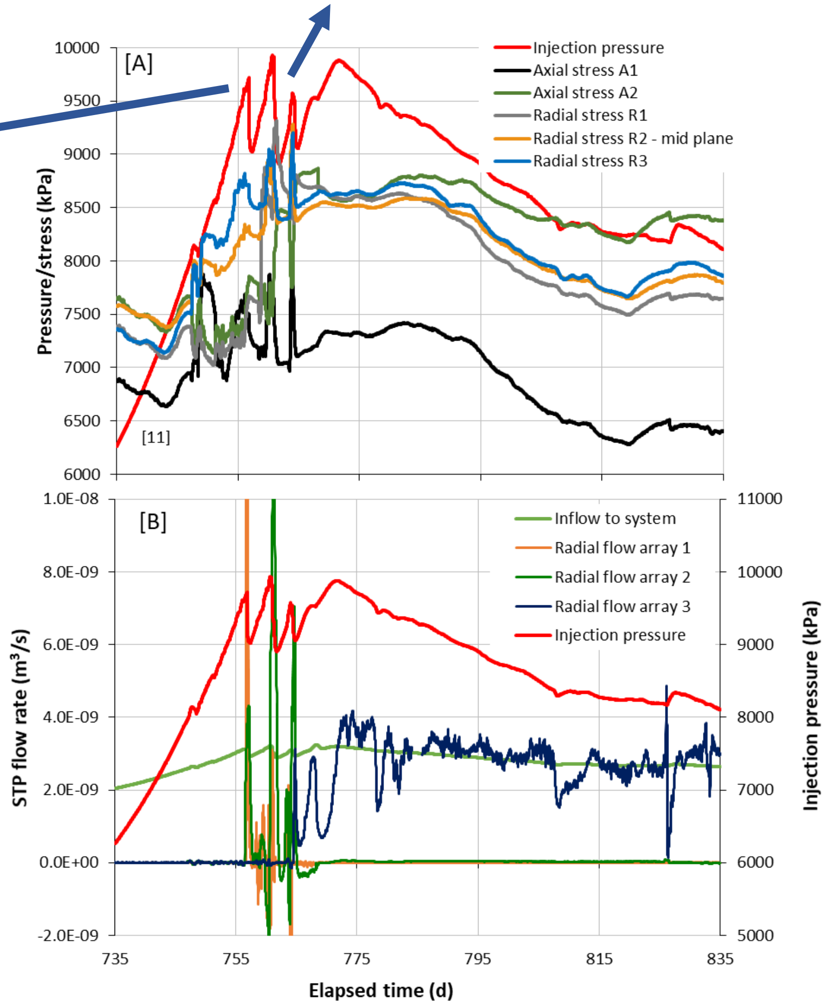

Fig.7. Experimental data from day 735 to day 835

Methodology

Modelling approaches

- Different modelling approaches have been developed through experimental data.
  1) Classical two-phase flow models
  2) Enhanced two-phase flow models
  3) Single-phase flow models
  4) Conceptual chaotic model

Table 3
Main properties of the modelling approaches that have been developed during the task (for both experiment 1 and experiment 2).

#	Model	Funding centre	Model type	Mechanical deformation	Hydraulic approach
1.	BGR/UFZ-E	BGR/UFZ	continuous	elasticity	two-phase
2.	CNSC-PD	CNSC	continuous	elastoplastic damage	two-phase
3.	KAERI-D	KAERI	continuous	elastic damage model	two-phase
4.	NCU/TPC-V	Taiwan Power Company	continuous	visco-elastic	two-phase
5.	UPC/Andra-ED	ANDRA	continuous	elasticity with dilatancy	two-phase with embedded fracture
6.	LBNL-D	US DOE	discontinuous	elastic damage and fractures	two-phase
7.	Quintessa/RWM-ECap	RWM	continuous	elasticity	single-phase

Table 4
Main numerical features of the modelling approaches that have been developed during the task (for both stage experiment 1 and stage experiment 2). See Appendix A for more details. Note that FE stands for Finite Element, FD stands for Finite Difference and FV for finite volume.

#	Model	Test	Software	Space discretisation method	Number of calibrated parameters
1.	BGR/UFZ-E	1,2	OpenGeoSys 5.8	FE	Not provided
2.	CNSC-PD	1,2	COMSOL Multiphysics® 5.4	FE	25
3.	KAERI-D	1	TOUGH2/FLAC3D	FD	5
		2	COMSOL Multiphysics®	FE	5
4.	NCU/TPC-V	1,2	THMC 7.1	FE	7
5.	UPC/Andra-ED	1,2	Code_bright 8.6	FE	11
6.	LBNL-D	1,2	TOUGH-RBSN	FV	Not provided
7.	Quintessa/RWM-ECap	1,2	QPAC 4.2	FV	12

1. Classical two-phase flow models: BGR/UFZ-E

➢ Mass conservation equation:

water phase

$$\frac{\partial \phi \rho_w S_w}{\partial t} + \phi \rho_w S_w \nabla \cdot \frac{\partial \boldsymbol{u}}{\partial t} + \nabla \cdot \boldsymbol{q}_w = 0$$

gas phase

$$\frac{\partial \phi \rho_g (1 - S_w)}{\partial t} + \phi (1 - S_w) \rho_g \nabla \cdot \frac{\partial \boldsymbol{u}}{\partial t} + \nabla \cdot \boldsymbol{q_g} = 0$$

ϕ: the porosity of the medium (-)
ρ_w: the density of *water* phase (kg/m^3)
ρ_g: the density of *gas* phase (kg/m^3)
S_w: the water saturation (-)
$\boldsymbol{q}_w$: the flow velocity of *water* (kg/m^2·s)
$\boldsymbol{q}_g$: the flow velocity of *gas* (kg/m^2·s)
u: the displacement vector (m)

➢ Momentum balance equation:

$$\nabla[\sigma' - \alpha(P_g - S_w P_c)\boldsymbol{I}] + \rho g = 0$$

σ': the effective stress tensor (Pa)
α: the Biot coefficient (-)
P_g: the gas pressure (Pa)
P_c: the capillary pressure (Pa)
$\boldsymbol{I}$: the identity tensor
ρ: the total density (kg/m^3)
g : the gravity acceleration (m/s^2)

➢ The pressure-dependent permeability relationship:

$$k = f(p_g) = \begin{cases} (1 + a p_g) k_{int} & , p_g \le p_{crit} \\ (b(p_g - p_{crit}) + 1 + a p_{crit}) k_{int}, & otherwise \end{cases}$$

p_{crit}: the critical value of gas pressure (Pa)
k_{int}: the intrinsic permeability tensor (-)
a, b: the calibrated constant parameter (m ^{2})

1. Classical two-phase flow models: CNSC-PD

- This hydraulic model is coupled to a non-linear poro-elastoplastic damage model that uses a modified extended Barcelona Basic Model.
- The Pall and Moshenin model is used for the intrinsic permeability:

$$k_{ij} = \frac{D_{VS}^2}{180} \frac{\varphi^3}{(1-\varphi)^2}$$

D_{VS}: the volume-surface mean diameter (m)
φ: the porosity (-)

1. Classical two-phase flow models: KAERI-D

- The classical multi-phase Darcy's law is used and combined with a mass balance equation for each component.
- This classical two-phase flow model is coupled to the elastic damage model proposed by Tang et al.
- The stress-strain relationship is divided into an elastic phase and a damage phase

$$Before\ gas\ breakthrough\ (elastic\ model):\quad \boldsymbol{\sigma}' = \mathbf{C} : \boldsymbol{\varepsilon}$$

$$After\ gas\ breakthrough\ (damage\ model):\ \boldsymbol{\sigma}' = (1 - D)\,\mathbf{C} : \boldsymbol{\varepsilon}$$

$$k_{int} = k_{int,undamaged} + k_{int,damaged}$$

1. Classical two-phase flow models: NCU/TPC-V

➢ Mass conservation equation:

water phase

Suk and Yeh(2007,2008);
Tsai and Yeh(2012,2013)

$$\frac{\partial \rho_\alpha \phi S_\alpha}{\partial t} + \nabla \cdot (\rho_\alpha \boldsymbol{V}_\alpha) + \nabla \cdot (\rho_\alpha \phi S_\alpha \boldsymbol{V}_s) = M^\alpha, \alpha \in \{L\} \qquad \sum_{\alpha=1}^{L} S_\alpha = 1$$

gas phase

Liu(2002,2006);
Liu et al.(2010)

$$\frac{\partial \rho_s \phi_s}{\partial t} + \nabla \cdot (\rho_s \phi_s \boldsymbol{V}_s) = 0$$

ρ_α: the density of α-th fluid phase (kg/m^3)
ϕ: the volume fraction (-)
S_α: the normalized saturation of α-th fluid phase (-)
$\boldsymbol{V}_\alpha$: the Darcy velocity of α-th fluid phase (m/s)
$\boldsymbol{V}_s$: the velocity of the solid (m/s)
M^α: the sum of the artificial source/sink rate of all species in α-th fluid phase (kg·m^3·s^{-1})

ρ_s: the density of the solid phase (kg/m^3)
$\boldsymbol{V}_s$: the velocity of the solid phase (m/s)
ϕ_s: the volume fraction of the solid phase with porosity $\phi = 1 - \phi_s$ (-)

1. Classical two-phase flow models: NCU/TPC-V

- Momentum balance equation:

$$-\nabla \cdot \mathbf{T} + \sum_{\alpha \in \{L\}} \nabla (S_{\alpha} p_{\alpha}) - \left[\sum_{\alpha \in \{L\}} \rho_{\alpha} \phi S_{\alpha} + \rho_s \phi_s \right] \boldsymbol{g} \nabla \mathbf{z} = -\phi_s \rho_s \frac{d^2 \boldsymbol{u}}{dt^2} \approx 0$$

T: the Cauchy stress tensor in the continuum mechanics (Pa)
p_{α}: the pressure of the α-th fluid phase (Pa)
$\boldsymbol{g}$: the gravitational acceleration (m/s^2)
z: the potential head (m)
$\boldsymbol{u}$: the displacement of the media (m)

$$k_{int} = k_{int,0} \left(\frac{1}{1 + (\phi_0 - \phi)} \right)^n$$

$k_{int,0}$: the reference intrinsic permeability
k_{int}: the intrinsic permeability
ϕ_0: the reference porosity
n: the fractional exponent depending on the particle size and packing structure

2. Enhanced two-phase flow models: UPC/Andra-ED

- UPC-Andra-ED is a heterogeneous continuous two-phase model, where the standard equations of balance of water, balance of gas and equilibrium of stresses are solved.
- This approach is characterized by the coupling of these standard equations to embedded fractures, which allow the representation of preferential pathways.

$$k_{int} = k_{matrix} + k_{fractures}$$

$$= \frac{k_0(1-\varphi_0)^2}{\varphi_0^3}\frac{\varphi^3}{(1-\varphi)^2} + \frac{b^3}{12a}$$

k_0: the reference permeability (m^2)
φ_0: the initial porosity (-)
φ: the porosity (-)
b: the fracture aperture (m)
a: the spacing between fractures (m)

2. Enhanced two-phase flow models: LBNL-D

- LBNL-D is a discontinuous two-phase flow model with mechanical deformation and fracture/damage processes.
- The Rigid-Body-Spring Network (RBSN), a lattice approach, is linked to the flow simulator (TOUGH2) in order to facilitate a discrete representation of fracture formations.
- Permeability is porosity dependent.

$$k = \begin{cases} \frac{k_0(1-\varphi_0)^2}{\varphi_0^3}\frac{\varphi^3}{(1-\varphi)^2}, if\ unfractured \\ k_0 + \frac{b^3}{12a} \quad , if\ fractured \end{cases}$$

k_0: the reference permeability (m^2)
φ_0: the initial porosity (-)
φ: the porosity (-)
b: the fracture aperture (m)
a: the element width (m)

3. Single-phase flow models: Quintessa

- In this model, gas transport through the system is modelled using Richards' equation.

$$\frac{\partial}{\partial t}(\theta_g \rho_g) = -\nabla \cdot (\rho_g \boldsymbol{q_g})$$

$$\text{, where } \boldsymbol{q_g} = -\frac{k_g}{\mu_g}(\nabla P_g + \rho_g g \nabla z)$$

θ_g: the volume fraction of the gas (-)
ρ_g: the density of gas (kg/m^3)
$\boldsymbol{q}_g$: the Darcy flux vector (m/s)

k_g: the intrinsic permeability for gas (m^2)
μ_g: the gas viscosity (Pa·s)
P_g: the gas pressure (Pa)
ρ_g: the gas density (kg·m^{-3})
g: the acceleration due to gravity (m·s^{-2})
z: the elevation (m)

- The gas permeability and gas porosity are made up of capillary(*cap*) and micro-scale deformation(*creep*) components:

$$k_g = k_{cap} + k_{creep} \qquad \theta_g = \theta_{cap} + \theta_{creep}$$

$$r = \begin{cases} r_0 + \gamma(\sigma_c(P_g, \sigma_{total}) - \sigma_{c0}), & \sigma_c > \sigma_{c0} \\ r_0, & otherwise \end{cases}$$

r_0: the reference capillary radius (m)
γ: the capillary compressibility (mPa^{-1})
σ_c: the excess stress for capillary opening (Pa)
P_g: the gas pressure (Pa)
σ_{total}: the total stress of the system
σ_{c0}: the reference pressure for capillary opening (Pa)

Results& Discussion

Experimental data

- Experimental data can be summarized by four key components:

  (i) quiescence phase

  (ii) gas breakthrough

  (iii) peak value

  (iv) a negative decay

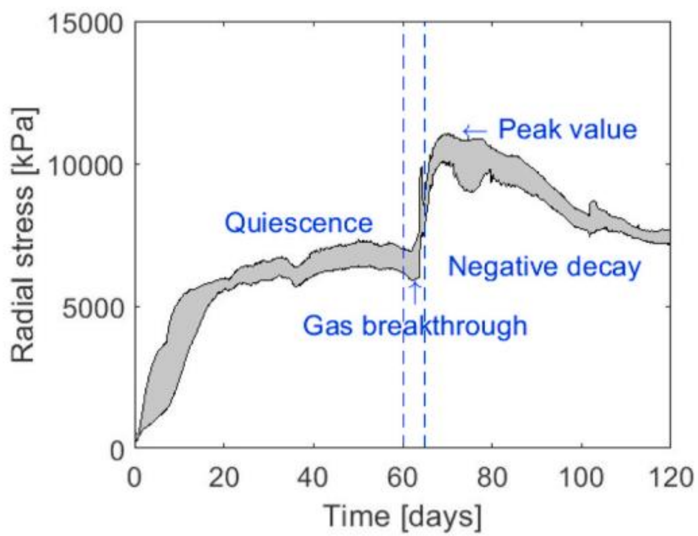

Fig.8. The radial stress of Test-1

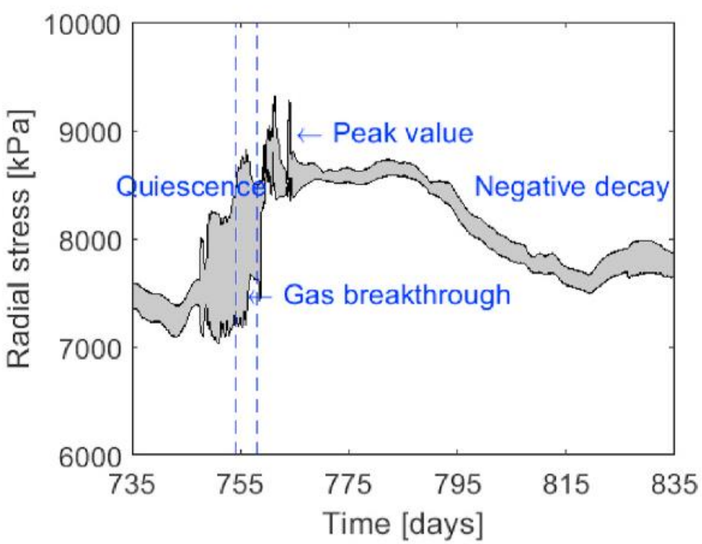

Fig.9. The radial stress of Test-2

Test-1 results

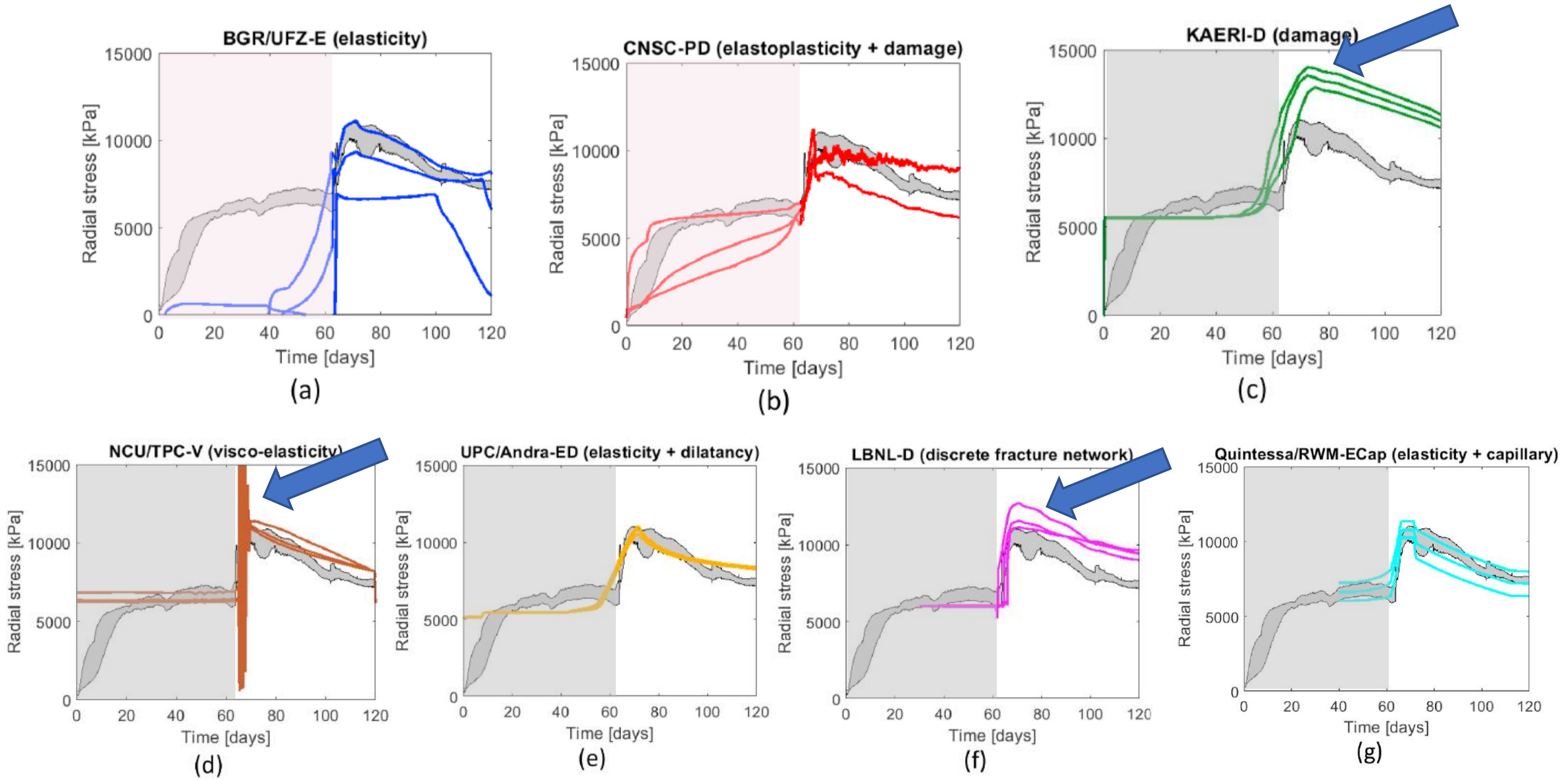

Fig.10. experimental versus numerical radial stresses with different teams

Test-2 results

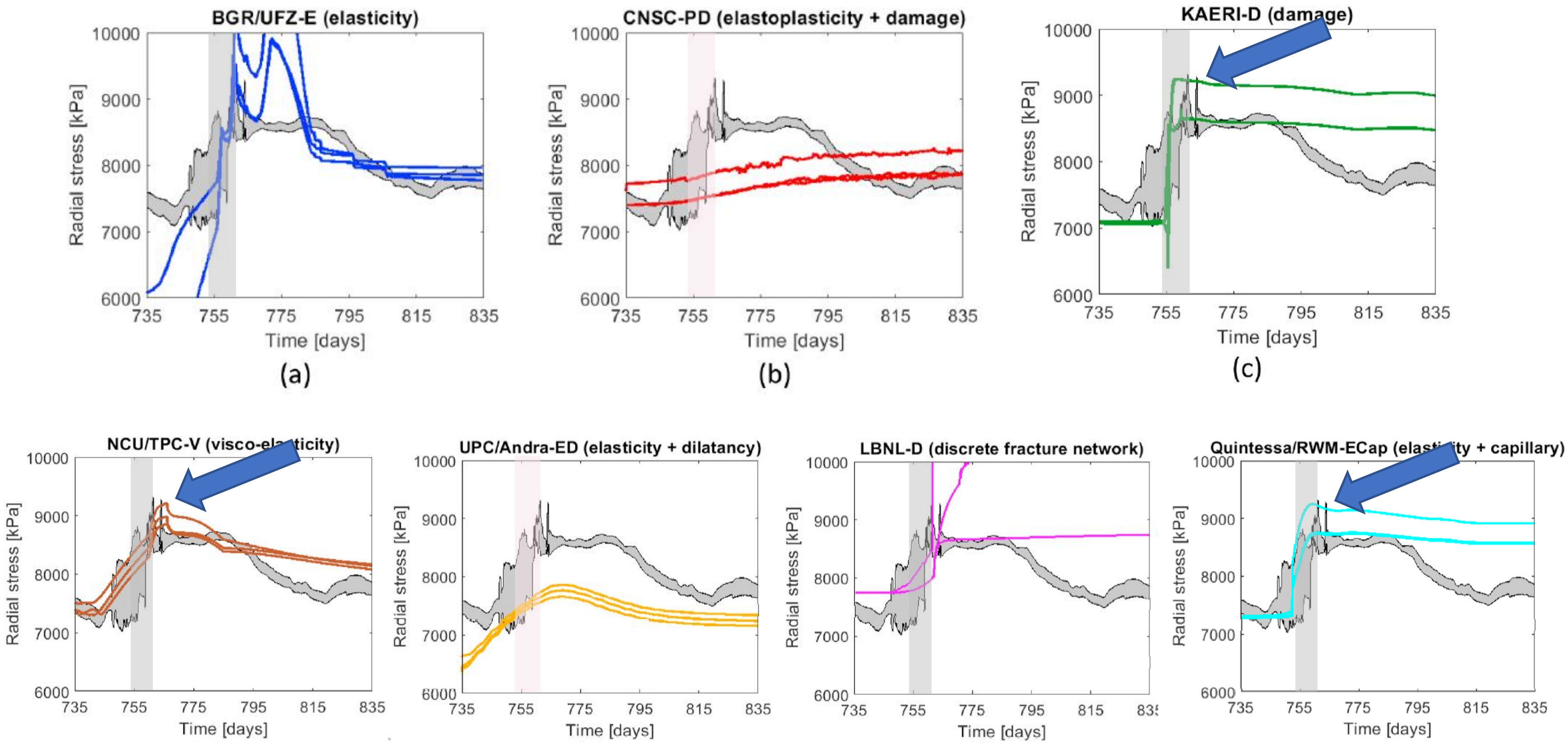

There are three times gas breakthrough events from the experimental data.
But most models only predict a single breakthrough event.
Hence, comparing the numerical predictions with the experimental results fairly is difficult since it is not obvious which of the experimental breakthroughs are best for the comparison.

Discussion

- Different codes and different test geometries have been used by the teams which makes it difficult to compare results directly across the teams.
- Model comparison is extremely difficult due to significant differences in the number of parameters that need to be calibrated in each model.

Table 14
Parameters for experiment 1.

	Model						
	BGR/UFZ-E	CNSC-PD	KAERI-D	NCU/TPC-V	UPC/Andra-ED	LBNL-D	Quintessa/RWM-ECap
Number of calibrated parameters	Not provided	25	5	7	11	Not provided	12
Elastic modulus (MPa)	307	307	307	307	307	307	307
Poisson's ratio (–)	0.4	0.4	0.4	0.4	0.4	0.4	0.4
Porosity (–)	0.44	Heterogeneity (mean: 0.44)	0.44	0.43	Heterogeneity (mean: 0.44)	0.44	Calculated
Biot's coefficient (–)	0.9	1	0.86		0.5	1	0.4
Dry density (kg/m^3)		1560	2700	1600	1512		
Intrinsic permeability of water (m^2)		3.4×10^{-21}	3.4×10^{-21}	3.4×10^{-22}~ 3.4×10^{-21}	Heterogeneous	3.4×10^{-21}	
			Klikoff[62]	et al.[43]			

These differences lead to models with very different degrees of freedom, and thus their fair comparison is a very complex task.
This paper just want to summarize and show the outcomes of different models.

Conclusions

Conclusions

- Seven different numerical models have been developed to simulate both Test-1 (1D gas flow) and Test-2 (spherical 3D gas flow). However, none of the models describe the full complexity of the physical processes observed in these experiments.
- Only two models considered heterogeneous distributions of material properties. However, it needs to be further explored and analyzed since it might provide one possible route to represent localization of flow.
- The models need to be up-scaling, since only experiments under controlled laboratory conditions were modelled, models that are tractable at repository scales are needed.

Thank you for your attention.